ARL4A acts with GCC185 to modulate Golgi complex organization

Yu-Chun Lin[1], Tsai-Chen Chiang[1], Yu-Tsan Liu[1], Yueh-Tso Tsai[1], Li-Ting Jang[1] and Fang-Jen S. Lee[1,2,*]

[1]Institute of Molecular Medicine, College of Medicine, National Taiwan University, Taipei, Taiwan
[2]Department of Medical Research, National Taiwan University Hospital, Taipei, Taiwan
*Author for correspondence (fangjen@ntu.edu.tw)

Accepted 4 July 2011
Journal of Cell Science 124, 4014–4026

doi: 10.1242/jcs.086892

Summary

ADP-ribosylation factor-like protein 4A (ARL4A) is a developmentally regulated member of the ARF/ARL GTPase family. The primary structure of ARL4A is very similar to that of other ARF/ARL molecules, but its function remains unclear. The trans-Golgi network golgin GCC185 is required for maintenance of Golgi structure and distinct endosome-to-Golgi transport. We show here that GCC185 acts as a new effector for ARL4 to modulate Golgi organization. ARL4A directly interacts with GCC185 in a GTP-dependent manner. Sub-coiled-coil regions of the CC2 domain of GCC185 are required for the interaction between GCC185 and ARL4A. Depletion of ARL4A reproduces the GCC185-depleted phenotype, causing fragmentation of the Golgi compartment and defects in endosome-to-Golgi transport. GCC185 and ARL4A localize to the Golgi independently of each other. Deletion of the ARL4A-interacting region of GCC185 results in inability to maintain Golgi structure. Depletion of ARL4A impairs the interaction between GCC185 and cytoplasmic linker-associated proteins 1 and 2 (CLASP1 and CLASP2, hereafter CLASPs) in vivo, and abolishes the GCC185-mediated Golgi recruitment of these CLASPs, which is crucial for the maintenance of Golgi structure. In summary, we suggest that ARL4A alters the integrity of the Golgi structure by facilitating the interaction of GCC185 with CLASPs.

Key words: ARF, CLASP, GTPase, Golgin, Trans-Golgi network

Introduction

Intracellular vesicle transport transfers membrane-bound and soluble cargo between organelles, setting up biosynthetic and/or secretory and endocytic pathways, which are essential for protein transport, cell signaling, cell migration and cell growth. It is well known that small GTPases of the Arf and Rab families play important roles in vesicular transport (D'Souza-Schorey and Chavrier, 2006; Stenmark, 2009).

The ADP-ribosylation factor-like (ARL) proteins are ~40–60% identical to ARF proteins and have diverse functions including regulation of membrane trafficking and microtubule formation by recruitment of specific effectors to the membrane to which they are bound (Burd et al., 2004). Among the more than 20 members of the ARL family in mammals, the expression levels of the three isoforms of ARL4 (i.e. ARL4A, ARL4C, ARL4D) are developmentally regulated, tissue specific and dependent on the stages of differentiation (Schürmann et al., 1994; Stephan et al., 1999; Lin et al., 2000; Lin et al., 2002). Disruption of the ARL4A gene in mice reduces the sperm count; in particular, ARL4A is involved in the early stages of spermatogenesis in adults (Schürmann et al., 2002). ARL4D and ARL4A, present at the plasma membrane, are able to recruit cytohesin-2 (ARNO) to promote ARF6 activation and modulate actin remodeling (Hofmann et al., 2007; Li et al., 2007). A previous study showed that ARL4A is distributed at the plasma membrane and in the cytoplasm (Li et al., 2007); however, the physiological roles of ARL4A in intracellular regions are still unknown.

Golgins belong to a family of coiled-coil proteins associated with the Golgi complex and are necessary for tethering events in membrane fusion and as structural supports for Golgi cisternae (Yoshino et al., 2003; Yoshino et al., 2005; Derby et al., 2007). There are four human golgins containing the Golgi-targeting GRIP domain, namely p230 (also known as golgin-245), golgin-97, GCC185 and GCC88 (Goud and Gleeson, 2010), all of which play roles in the organization of the Golgi structure and intracellular vesicle transport (Yoshino et al., 2003; Yoshino et al., 2005; Derby et al., 2007). The structural integrity of the Golgi complex is known to be dependent upon microtubule polymerization and microtubule–Golgi interaction (Goud and Gleeson, 2010). GCC185 has been shown to interact with the CLASP family of microtubule-binding proteins to recruit them to the Golgi, providing a microtubule–Golgi interaction to maintain the structural integrity of the Golgi complex (Efimov et al., 2007; Miller et al., 2009).

In this study, we investigated the intracellular role of ARL4A and its interaction with golgin GCC185, which was identified through a yeast two-hybrid assay. We discovered a new role for ARL4A in the maintenance of Golgi structure and endosome-to-Golgi transport. We demonstrate that a portion of ARL4A is localized at the trans-Golgi network (TGN) and bound directly to the coiled-coil motif of GCC185 in a GTP-dependent manner. Depletion of ARL4A reproduces the phenotype of GCC185 depletion, causing fragmentation of the Golgi compartment and defects in endosome-to-TGN membrane transport. Deletion of the ARL4A-interacting sub-coiled-coil region of GCC185 results in an inability to maintain Golgi structure and endosome-to-Golgi transport. Furthermore, depletion of ARL4A impairs the interaction between GCC185 and cytoplasmic linker-associated

proteins 1 and 2 (CLASP1 and CLASP2, hereafter CLASPs) in vivo and abolishes the GCC185-mediated Golgi recruitment of CLASPs. Our data indicate that ARL4A acts with its new effector GCC185 to modulate TGN organization.

Results

ARL4A directly interacts with GCC185 in a GTP-dependent manner

To identify potential effectors of ARL4A, we used ARL4A Q79L, a putative GTP-bound form of ARL4A, as bait to screen a human fetal brain cDNA library in a yeast two-hybrid system. We identified several candidates, of which three were a fragment (residues 414–733) of GCC185, a golgin that localizes to the TGN.

Secondary structure prediction algorithms revealed distinct regions with high coiled-coil probability along the length of GCC185: CC1, CC2, CC3, the C-terminal domain (CTD) and C270 (including the GRIP domain; Fig. 1A) (Hayes et al., 2009). To determine the specific domains of GCC185 responsible for its interaction with the three ARL4 family members, we generated a series of constructs spanning the length of GCC185 and tested for their ability to interact with ARL4 in yeast two-hybrid assays (Fig. 1B). Only the CC2 domain of GCC185 interacted with ARL4A. When the other two ARL4 family members, ARL4C and ARL4D, were examined for their interaction with the GCC185 domains, no interaction with any of the domains was observed. In addition, the CC2 domain interacted with ARL4A Q79L but not with the GTP-binding-defective mutant, ARL4A

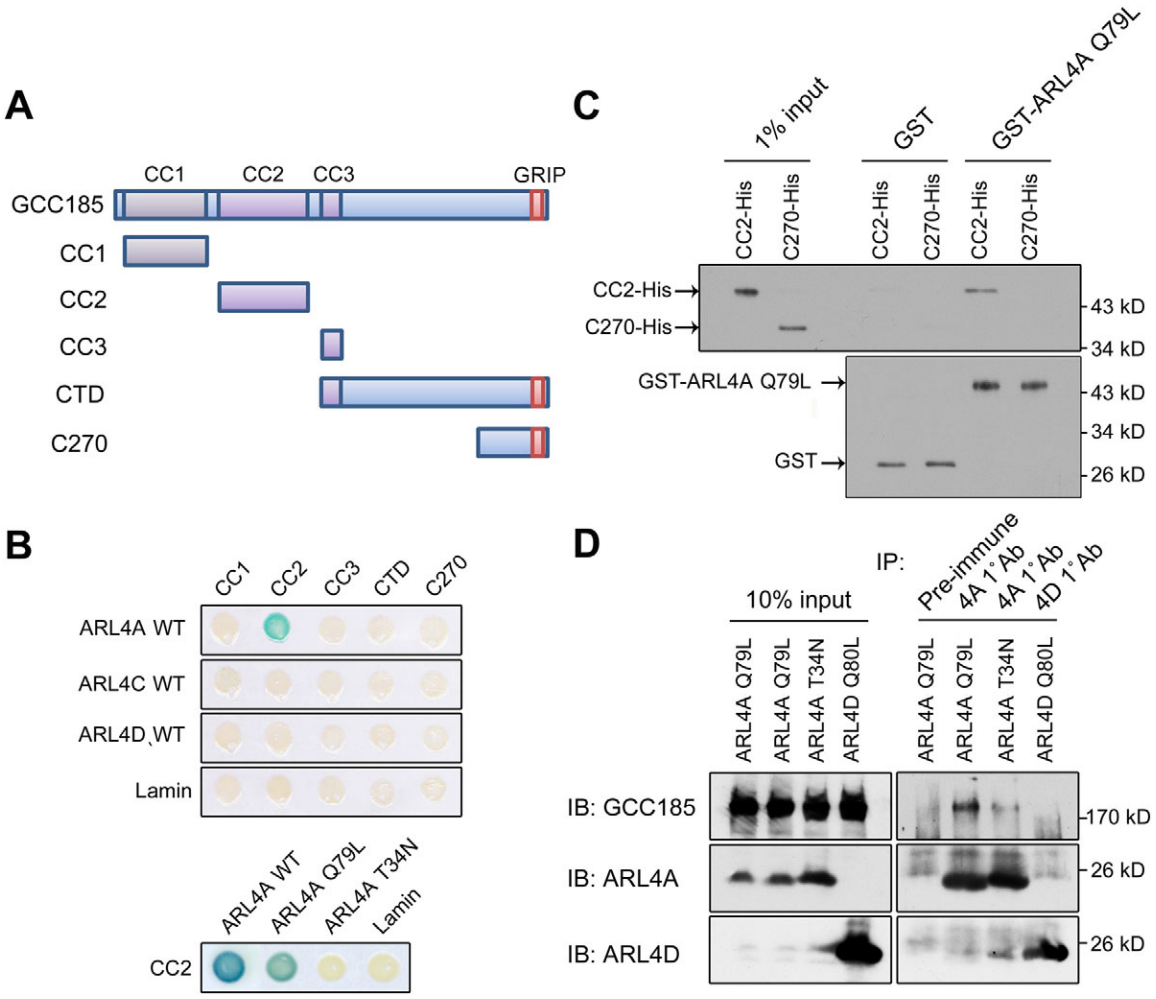

Fig. 1. ARL4A interacts directly and specifically with GCC185. (**A**) Schematic representation of GCC185 and its fragments. GCC185 contains three predicted coiled-coil domains (CC1, CC2 and CC3), the C-terminal domain fragment (CTD) and the C270 fragment. (**B**) ARL4A interacts with the CC2 domain of GCC185 in a yeast two-hybrid system. ARL4A WT, ARL4A Q79L, ARL4A T34N, ARL4C WT or ARL4D WT fused to the LexA DNA-binding domain were co-transformed with the indicated coiled-coil domains and fragments of GCC185 fused to the GAL4-activation domain into yeast strain L40, and the transformants were tested for their ability to express β–galactosidase. Lamin was used as a negative control. (**C**) Purified CC2–His or C270–His was incubated with either GST or GST–ARL4A Q79L immobilized on glutathione beads. Bead-bound His-tagged proteins were probed using anti-His antibody. Equal inputs of GST fusion proteins used in the assay and detected by GST antibody are shown on the bottom panel. (**D**) Interaction between ARL4A and GCC185 in vivo. HeLa cells expressing ARL4A Q79L, ARL4A T34N or ARL4D Q80L were lysed and incubated with equal amounts of preimmune serum, anti-ARL4A antibody or anti-ARL4D antibody. Immune complexes were isolated using protein-A–agarose, and bound proteins were analyzed by immunoblotting with anti-GCC185, anti-ARL4A or anti-ARL4D antibody. Ten percent of each cell lysate (input) was loaded to show expression levels.

T34N (Fig. 1B), suggesting that ARL4A specifically interacts with the CC2 domain of GCC185 in a GTP-dependent manner.

To test whether ARL4A directly bind to GCC185, we generated and purified histidine-tagged CC2 and C270 domains, as well as GST-fused ARL4A Q79L. We found that GST–ARL4A Q79L pulled down CC2–His, but not C270–His (Fig. 1C), indicating that the CC2 domain of GCC185 directly interacts with ARL4A. We next examined whether ARL4A interacts with GCC185 in vivo. Lysates of HeLa cells expressing ARL4A Q79L, ARL4A T34N or ARL4D Q80L, a putative GTP-bound form of ARL4D, were immunoprecipitated with pre-immune serum, anti-ARL4A or anti-ARL4D antibodies, and analyzed by immunoblotting. As shown in Fig. 1D, endogenous GCC185 was co-immunoprecipitated with ARL4A Q79L, but not with ARL4A T34N or ARL4D Q80L. These results demonstrate that ARL4A specifically interacted with the CC2 domain of GCC185 in a GTP-dependent manner.

Internal sub-coiled-coil regions of the CC2 domain of GCC185 are required for the interaction between GCC185 and ARL4A

We continued to define the ARL4A-binding region within the CC2 domain of GCC185. The coiled-coil structure of GCC185 is important for its interaction with other partners (Sinka et al., 2008; Hayes et al., 2009). Structure prediction of the CC2 domain indicates that there are six sub-coiled-coil regions (CC2a, CC2b, CC2c, CC2d, CC2e and CC2f; Fig. 2A). The interactions between these sub-coiled-coil regions and ARL4A were investigated using a yeast two-hybrid assay. Deletion of the CC2a and CC2f regions in a construct encoding GCC185(500–714) did not abolish the interaction between the CC2 domain and ARL4A (Fig. 2B). However, elimination of any of the four internal coiled-coil regions did abolish the interaction (Fig. 2B). Of the four sub-coiled-coil domains within the CC2 domain, CC2b is the most conserved region in mammals. To confirm that

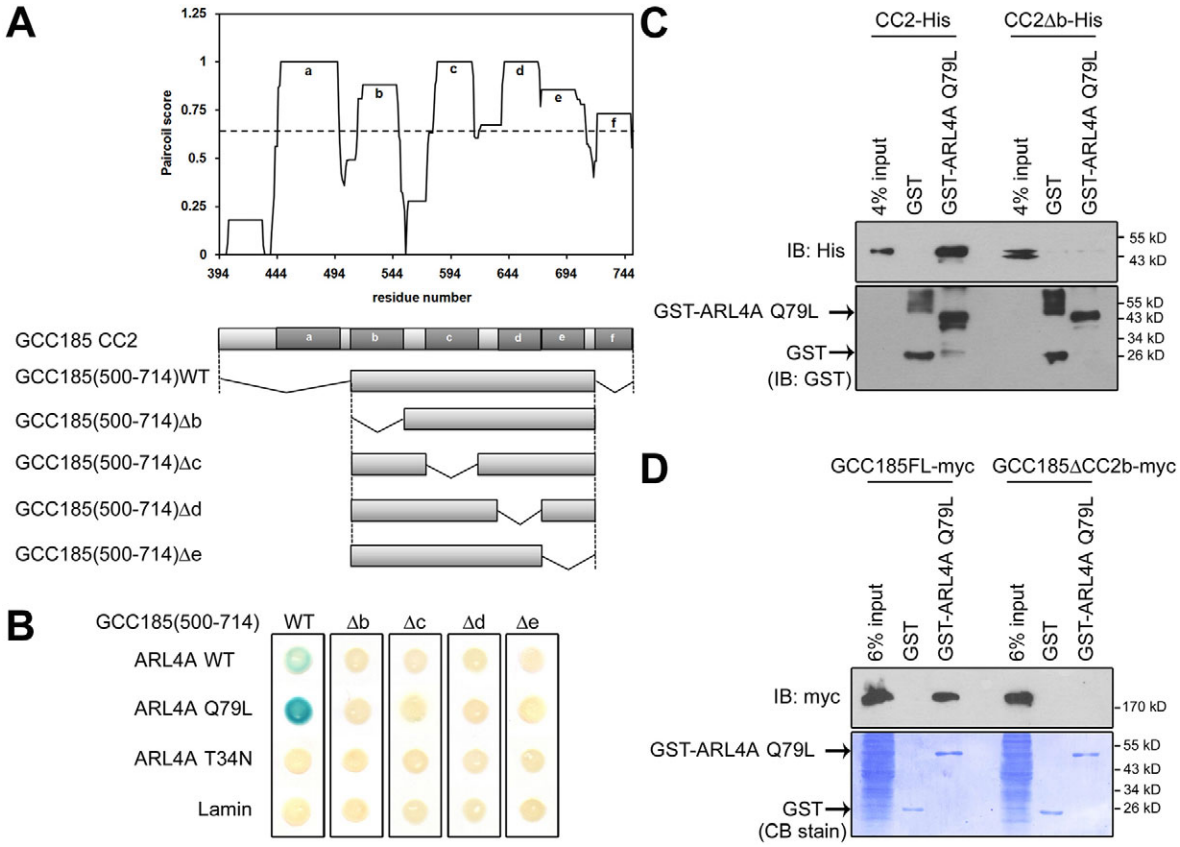

Fig. 2. The internal sub-coiled-coil regions of the CC2 domain of GCC185 are required for the ARL4A–GCC185 interaction. (**A**) Predicted structure of the CC2 domain in GCC185. Potential coiled-coil regions (score >0.6) in the CC2 domain of GCC185 were predicted using the Paircoil program and referred to as CC2a, CC2b, CC2c, CC2d, CC2e and CC2f (naming from the N-terminus to the C terminus of the CC2 domain). A schematic representation of the CC2 domain and its deletion mutants is shown below. (**B**) ARL4A interacts with the internal four sub-coiled-coil regions of the CC2 domain in a yeast two-hybrid system. ARL4A WT, ARL4A Q79L or ARL4A T34N fused to LexA DNA-binding domain were co-transformed with deletion mutants of the CC2 domains fused to a Gal4-activating domain into yeast strain L40, and the transformants were tested for their ability to express β-galactosidase. Lamin was used as a negative control. (**C**) Interaction between ARL4A and the CC2Δb fragment. Purified CC2–His or CC2Δb–His was incubated with either GST or GST–ARL4A Q79L immobilized on glutathione beads. Bead-bound His-tagged proteins were probed using an anti-His antibody. Equal inputs of the GST fusion proteins used in the assay were validated using a GST antibody. (**D**) Interaction between ARL4A and GCC185ΔCC2b. Lysates from HEK293T cells expressing GCC185FL or GCC185ΔCC2b were incubated with either GST or GST–ARL4A Q79L immobilized on glutathione beads. Bead-bound GCC185 was probed using an anti-myc antibody. Six percent of the cell lysate (input) was probed in each of the experiments. Equal inputs of GST and GST–ARL4A Q79L used in the assay were validated by Coomassie Blue staining.

CC2b is required for the ARL4A–GCC185 interaction, an in vitro GST pull-down assay was performed to determine the interaction between either the CC2Δb fragment or full-length GCC185ΔCC2b and ARL4A Q79L (Fig. 2C,D). GST–ARL4A Q79L pulled down more of the wild-type CC2 domain than the CC2Δb fragment (Fig. 2C). Moreover, GST–ARL4A Q79L pulled down more GCC185FL–myc than GCC185ΔCC2b–myc. GST immunoprecipitated as a control failed to pull down either GCC185FL–myc or GCC185ΔCC2b–myc (Fig. 2D). These data indicate that sub-coiled-coil CC2b within the CC2 domain is required for the interaction between ARL4A and GCC185.

ARL4A colocalizes with GCC185 at the TGN

To examine whether ARL4A, like GCC185, localizes to the Golgi complex, we determined the intracellular localization of ARL4A by immunofluorescence staining. Our ARL4A antibodies were unable to detect endogenous ARL4A by immunoblotting or immunofluorescence staining, therefore, we expressed ARL4A, ARL4A Q79L and ARL4A T34N, and determined their intracellular localization in HeLa cells. As indicated, ARL4A colocalized with a plasma membrane marker in a punctate pattern in intracellular areas and partially colocalized with the following proteins: the trans-Golgi marker p230, the early endosome marker EEA1, the late endosome marker LAMP1 and the recycling endosome marker transferrin receptor. However, ARL4A did not colocalize with the *cis*-Golgi marker GM130 or the mitochondrial marker cytochrome *c* (supplementary material Fig. S1A). ARL4A Q79L presented a pattern similar to that of wild-type ARL4A (ARL4A WT) and colocalized with p230; whereas, ARL4A T34N distributed diffusely throughout the cytoplasm and did not colocalize with p230 (supplementary material Fig. S1B). We also examined the subcellular localization of ARL4C WT and ARL4D WT in transiently transfected cells. As shown in supplementary material Fig. S1C, ARL4C WT and ARL4D WT did not colocalize with p230. These results indicate that ARL4A is the only member of the ARL4 subfamily that localizes at the TGN in a GTP-dependent manner.

We further examined whether ARL4A colocalizes with GCC185 at the TGN. As shown in Fig. 3, ARL4A WT and ARL4A Q79L colocalized with GCC185FL–myc in the perinuclear TGN region to a much great extent than ARL4A T34N, ARL4C WT or ARL4D WT. Thus, these data indicate that ARL4A in part colocalizes with GCC185 at the TGN.

ARL4A is required for the maintenance of the structural integrity of the Golgi complex

To explore whether ARL4A, like GCC185, contributes to Golgi organization, we depleted ARL4A in HeLa cells using short hairpin RNAs (shRNA) and enriched the shRNA-transfected cells by puromycin selection. We utilized real-time RT-PCR to verify the successful silencing of ARL4A expression. The mRNA level of ARL4A in *ARL4A* shRNA-transfected cells was substantially lower than that in control luciferase shRNA-transfected cells (supplementary material Fig. S2A, and data not shown). The Golgi structure in ARL4A-depleted cells was observed by immunostaining with the trans-Golgi marker p230 and the *cis*-Golgi marker GM130. In cells transfected with control luciferase shRNA, p230 and GM130 retained their typical juxtanuclear Golgi staining pattern (Fig. 4A). By contrast, p230 was distributed in punctate fragments scattered throughout the cytoplasm in ARL4A-depleted cells (Fig. 4A). In ARL4A-depleted cells, GM130 also had a punctate pattern and localized closely with the p230-positive structures, suggesting that the

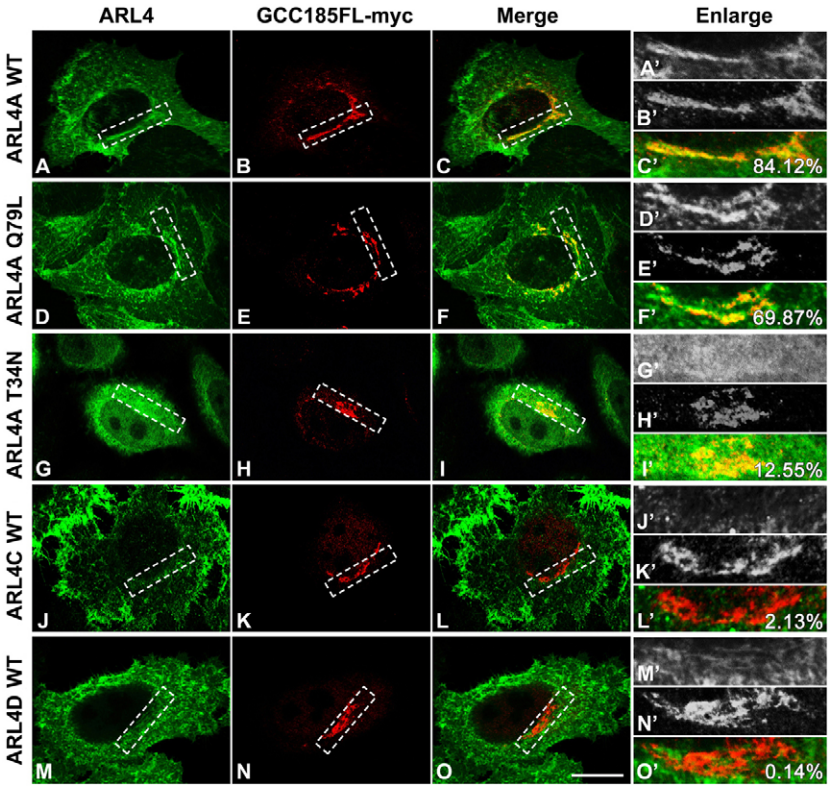

Fig. 3. ARL4A specifically colocalizes with GCC185 in a nucleotide-dependent manner. (**A–O**) HeLa cells grown on cover slips were transiently co-transfected with GCC185 and constructs encoding ARL4A WT, ARL4A Q79L, ARL4A T34N, ARL4C WT or ARL4D WT. Twenty-four hours after transfection, cells were fixed, permeabilized and processed for staining with antibodies against ARL4A, ARL4C, ARL4D or myc. (**A′–O′**) Magnified views of the boxed regions are shown in A′–O′. The level of colocalization between ARL4 and GCC185FL–myc was analyzed by Metamorph software and shown in merge images. Scale bar: 15 μm.

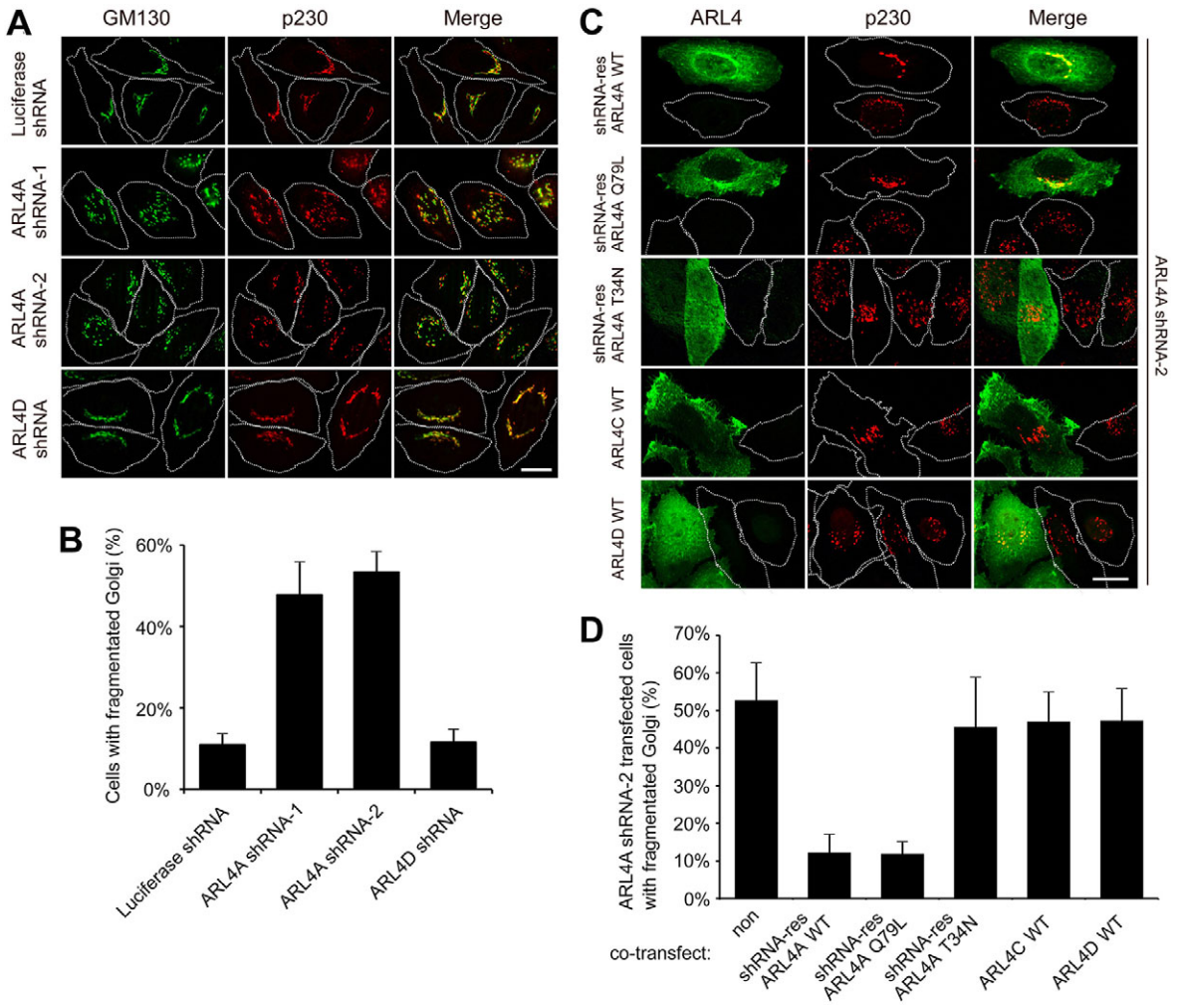

Fig. 4. ARL4A maintains the Golgi structure in a nucleotide-dependent manner. (**A**) Depletion of ARL4A disrupts p230 and GM130 staining. HeLa cells transfected with the indicated shRNAs were grown for 72 hours in the presence of puromycin before being fixed and stained with anti-p230 and GM130 antibodies followed by the appropriate Alexa-Fluor-conjugated antibodies. Scale bar: 20 μm. (**B**) Quantification of the data shown in A. Values are means ± s.d. of three independent experiments. (**C**) ARL4A function is nucleotide dependent. Cells were transfected with *ARL4A* shRNA-2 and subjected to puromycin selection for 72 hours. After 48 hours of shRNA treatment, cells were transfected with plasmids encoding the indicated proteins. The Golgi complex was detected using mouse anti-p230 antibodies. ARL4 construct expression was detected using antibodies against ARL4A, ARL4C or ARL4D. Scale bar: 20 μm. (**D**) Quantification of the data shown in C. Values are means ± s.d. of three independent experiments.

individual Golgi fragments present throughout the cytoplasm of ARL4A-depleted cells contained the *trans*- and *cis*-cisternae (Fig. 4A). Quantification of cells with fragmented Golgi confirmed that depletion of ARL4A caused Golgi fragmentation (Fig. 4B). To rule out the possibility that Golgi fragmentation resulted from puromycin treatment, we examined Golgi structure in *ARL4A*-shRNA–GFP-transfected cells without puromycin treatment. As expected, depletion of ARL4A by *ARL4A*-shRNA–GFP also caused Golgi fragmentation (supplementary material Fig. S2E).

We also examined whether depletion of ARL4D causes Golgi fragmentation. Endogenous ARL4D protein in *ARL4D*-shRNA-transfected cells was substantially lower than that in luciferase-shRNA-transfected cells (supplementary material Fig. S2B). As can be seen in Fig. 4A, p230 and GM130 were largely unaffected in ARL4D-depleted cells. Moreover, there was no detectable *ARL4C* mRNA in HeLa cells (data not shown). Thus, our data indicate that ARL4A, but not ARL4C or ARL4D, is required for the maintenance of Golgi structure.

To explore whether ARL4A maintenance of the Golgi structure is nucleotide dependent, we carried out a complementary gene rescue study in ARL4A-depleted cells. We engineered a hairpin-insensitive cDNAs of ARL4A WT, ARL4A Q79L or ARL4A T34N harboring synonymous mutations (see Materials and Methods). As shown in Fig. 4C, p230 was distributed in fragments scattered throughout the cytoplasm of ARL4A-depleted cells. Expression of the short hairpin RNA (shRNA)-resistant ARL4A WT and ARL4A Q79L constructs restored normal Golgi morphology. By contrast, the shRNA-resistant ARL4A T34N, ARL4C WT and ARL4D WT constructs were unable to reverse the fragmented Golgi phenotype (Fig. 4C). Quantification of cells with Golgi fragmentation confirmed that ARL4A WT and ARL4A Q79L restored normal Golgi morphology in ARL4A-depleted cells

(Fig. 4D). These data indicate that the effect of ARL4A depletion on Golgi structure can be specifically rescued by ARL4A and that the effect of ARL4A on maintenance of Golgi structure is nucleotide dependent.

ARL4A depletion impairs distinct endosome-to-Golgi transport

Derby et al. showed that GCC185 depletion lead to a block in Shiga toxin B-subunit (STxB) trafficking and a perturbation in the distribution of the mannose-6-phosphate receptor (M6PR), which occurred in parallel with Golgi fragmentation (Derby et al., 2007). However, the retrograde transport of TGN38 and cholera toxin B protein (CTxB) and anterograde transport of vesicular stomatitis virus G protein (VSVG) are GCC185 independent (Derby et al., 2007; Ganley et al., 2008). We next examined whether ARL4A depletion, impairs the intracellular vesicle transport of STxB and M6PR, as does depletion of GCC185. STxB is transported from the plasma membrane to the endoplasmic reticulum through endocytic compartments and the Golgi complex (Mallard et al., 1998). After incubation for 40 minutes at 37℃, the majority of internalized STxB was found in the Golgi region of the control luciferase-shRNA-transfected cells (Fig. 5A). By contrast, STxB was not able to reach the fragmented Golgi in ARL4A-depleted cells, and remained predominantly associated with peripheral structures throughout the cytoplasm (Fig. 5A). Moreover, the internalized STxB colocalized with p230 in ARL4D-depleted cells (Fig. 5A). Quantification of cells with dispersed STxB confirmed a block of STxB transport to Golgi in ARL4A-depleted cells (Fig. 5B). Very low levels of colocalization between EEA1 or LAMP1 and STxB were found in ARL4A-depleted cells, indicating that dispersed STxB did not localize to early or late endosomes (Fig. 5C). Quantification of these data showed that dispersed STxB predominantly colocalized with transferrin-labeled structures, which are considered to be recycling endosomes (Fig. 5C,D). These data indicate that ARL4A is required for the transport of STxB from recycling endosomes to the Golgi.

We further analyzed the intracellular distribution of the cation-independent M6PR in ARL4A-depleted cells. Similar to previous reports (Reddy et al., 2006; Derby et al., 2007), M6PR was found to be distributed in perinuclear late endosomes and, to a lesser extent, in the TGN of luciferase-shRNA-transfected control cells (Fig. 5E). In ARL4A-depleted cells, M6PR lost its perinuclear localization and was detected in more dispersed, vesicular structures; by contrast, the distribution of M6PR was not affected in ARL4D-depleted cells (Fig. 5E). Quantification of cells with dispersed M6PR confirmed that depletion of ARL4A increased the number of cells with dispersed M6PR (Fig. 5F). Very rarely did EEA1 or LAMP1–RFP colocalize with M6PR in ARL4A-depleted cells, indicating that dispersed M6PR did not localize in early or late endosomes (Fig. 5G). M6PR recycling between late endosomes and the TGN requires Rab9 GTPase and its effectors (Ghosh et al., 2003). To determine whether the M6PR-containing accumulated vesicles contained Rab9 protein, ARL4A-depleted cells were co-stained with Rab9 antibody and fluorescein-conjugated M6PR antibody. As shown in Fig. 5G,H, the dispersed M6PR mainly localized to Rab9-positive structures. These data indicate that ARL4 depletion leads to a perturbation of the distribution of M6PR and dispersed M6PR in Rab9-positive transport intermediates that are unable to target to the Golgi complex.

Previous studies have shown that retrograde transport of TGN38 and CTxB and anterograde transport of VSVG are GCC185 independent (Derby et al., 2007; Ganley et al., 2008). We further examined the effect of ARL4A depletion on these routes of vesicular transport. As shown in supplementary material Figs S3–S5, the internalization of TGN38 and CTxB and transport of VSVG were not impaired in ARL4A-depleted cells. Together, our data showed that ARL4A, like GCC185, is involved in distinct endosome-to-Golgi transport and suggest that anterograde transport is functional in ARL4A-depleted cells.

GCC185 and ARL4A localize to the Golgi, independently of each other

We have shown that ARL4A has physical and functional interaction with GCC185 (Figs 1–5). Does GCC185 function as an ARL4A effector and get recruited to the Golgi upon ARL4A activation? Or does GCC185 facilitate the Golgi localization of activated ARL4A? We examined whether ARL4A regulates the Golgi localization of GCC185 and vice versa by examining the localization of GCC185 in ARL4A-depleted cells or ARL4A localization in GCC185-depleted cells. HeLa cells transfected with shRNAs targeting GCC185 showed considerably reduced endogenous levels of GCC185 (supplementary material Fig. S2C). The Golgi (labeled by p230) was fragmented in GCC185-depleted cells, and ARL4A was still observed in the fragmented Golgi (Fig. 6A), indicating that localization of ARL4A to the Golgi is independent of GCC185. In ARL4A-depleted cells, GCC185 was distributed in the fragmented Golgi throughout the cytoplasm, indicating that the Golgi localization of GCC185 is independent of ARL4A (Fig. 6A). We also examined whether GCC185 or ARL4 depletion affects the subcellular distribution of ARL4A or GCC185 by cytosol–membrane fractionation analysis. As indicated, ARL4A depletion did not affect the protein expression level or subcellular distribution of GCC185, and GCC185 depletion did not affect the distribution of ARL4A (Fig. 6B,C). Our data indicate that the localization of GCC185 to the Golgi is ARL4A independent and vice versa.

Deletion of the ARL4A-interacting region of GCC185 results in inability to maintain Golgi structure and modulate endosome-to-Golgi transport

To explore the significance of the interaction between ARL4A and GCC185 in modulating cellular processes, we employed GCC185 mutants that were unable to interact with ARL4A, and evaluated their effects on the integrity of Golgi morphology and intracellular trafficking pathways. We performed gene rescue experiments in which we overexpressed GCC185FL, GCC185ΔCC2, or GCC185ΔCC2b in GCC185-depleted cells. Consistent with a previous study (Hayes et al., 2009), deletion of the CC2 domain or the CC2b domain did not affect the trans-Golgi localization of GCC185 (supplementary material Fig. S6B). As shown in Fig. 7, expression of exogenous GCC185FL-myc, but not GCC185ΔCC2 or GCC185ΔCC2b, in GCC185-depleted cells restored normal Golgi morphology. Quantification of cells with fragmented Golgi confirmed that overexpression of GCC185FL, but not GCC185ΔCC2 or GCC185ΔCC2b, in GCC185-depleted cells decreased the population of cells with fragmented Golgi (Fig. 7B). In addition, GCC185FL, but not GCC185ΔCC2 or GCC185ΔCC2b, restored defects of M6PR recycling in GCC185-depleted cells (supplementary material Fig. S7). These data indicate that the ARL4A-binding domain within

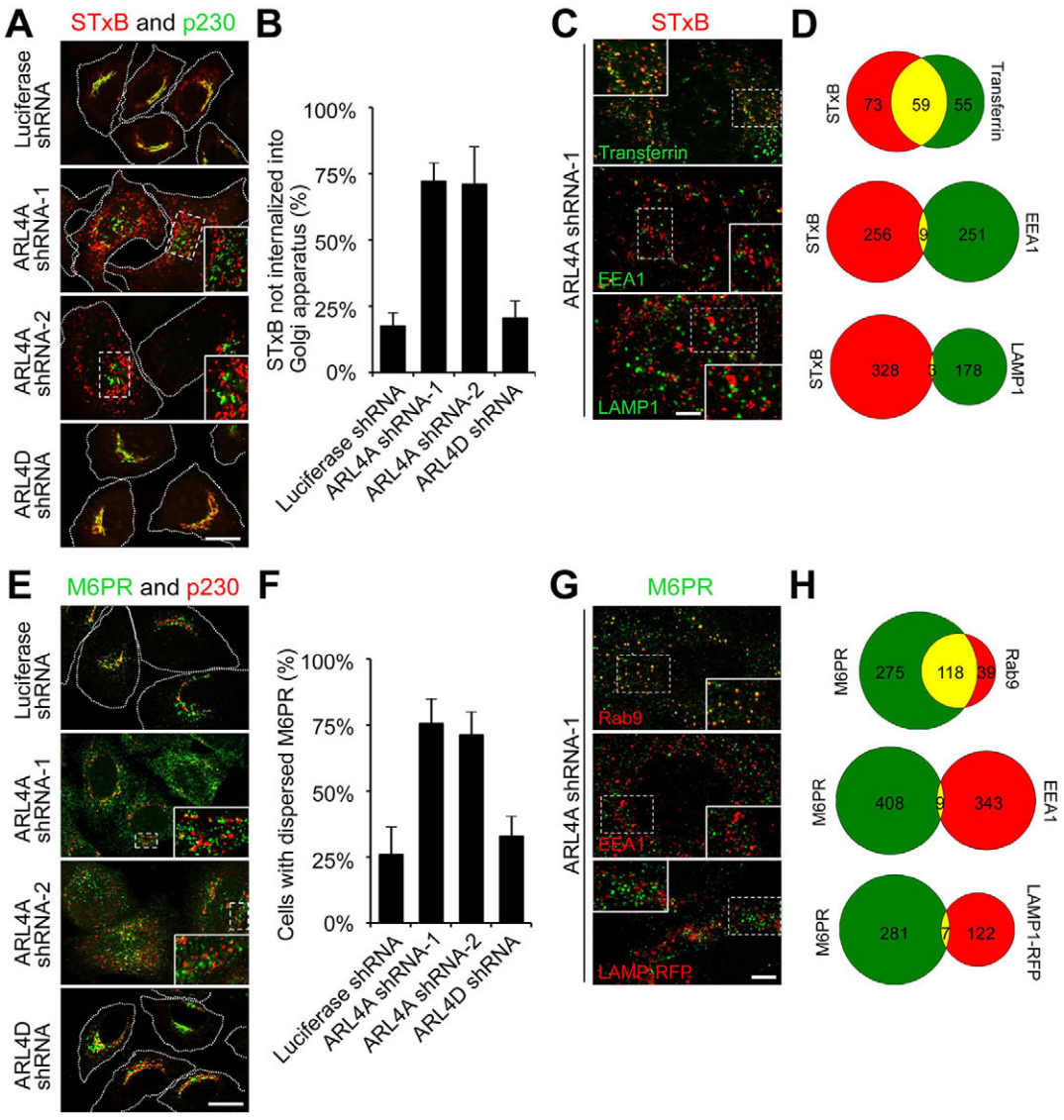

Fig. 5. ARL4A depletion impairs trafficking of STxB and perturbs the distribution of M6PR. (**A**) Control luciferase shRNA-, *ARL4A* shRNA-1-, *ARL4A* shRNA-2-, or *ARL4D* shRNA-transfected cells were incubated with Cy3-conjugated STxB for 30 minutes on ice and then incubated at 37°C for 40 minutes, followed by fixation and immunostaining with monoclonal anti-p230 antibodies and appropriate secondary antibodies. Magnified views of the boxed regions are shown in the insets. Scale bar: 20 µm. (**B**) Quantification of the data shown in A. Values are means ± s.d. of three independent experiments. (**C**) *ARL4A* shRNA-1-transfected cells were allowed to internalize Cy3-conjugated STxB and Alexa-Fluor-488–transferrin for 40 minutes. Cells were then fixed, permeabilized and stained with antibodies against EEA1 or LAMP1, followed by appropriate secondary antibodies. Magnified views of the boxed regions are shown in the insets. Scale bar: 5 µm. (**D**) Venn diagrams showing the quantification of the colocalization of transferrin, EEA1 or LAMP1 and STxB in *ARL4A* shRNA-1-transfected cells. (**E**) HeLa cells transfected with the indicated shRNA constructs were grown for 72 hours, fixed, permeabilized and stained with antibodies against M6PR and p230 followed by the appropriate secondary antibodies. Magnified views of the boxed regions are shown in the insets. Scale bar: 20 µm. (**F**) Quantification of the data shown in E. Values are means ± s.d. of three independent experiments. (**G**) HeLa cells transfected with *ARL4A* shRNA-1 and subjected to puromycin selection for 72 hours. After 48 hours of shRNA treatment, ARL4A-depleted cells were transfected with a construct encoding LAMP1–RFP. Cells were then fixed, permeabilized and processed for staining with fluorescently conjugated M6PR, Rab9 or EEA1 antibodies followed by the appropriate secondary antibodies. Magnified views of the boxed regions are shown in the insets. Scale bar: 5 µm. (**H**) Venn diagrams showing the quantification of the colocalization of Rab9, EEA1 or LAMP1-RFP and M6PR in *ARL4A*-shRNA-1-transfected cells.

GCC185 is involved in maintenance of Golgi structure and endosome-to-Golgi transport.

ARL4A is involved in GCC185-dependent recruitment of CLASPs to the Golgi membrane

It has been suggested that GCC185 modulates Golgi morphology through regulation of microtubule dynamics by recruiting CLASPs, a family of microtubule plus-end binding proteins, to the Golgi membrane (Efimov et al., 2007; Miller et al., 2009). GCC185 depletion results in exclusion of CLASPs from the TGN, leading to Golgi fragmentation (Derby et al., 2007; Efimov et al., 2007; Miller et al., 2009). We first examined the Golgi localization of endogenous CLASPs in cells lacking GCC185, ARL4A or ARL4D by immunofluorescence staining and

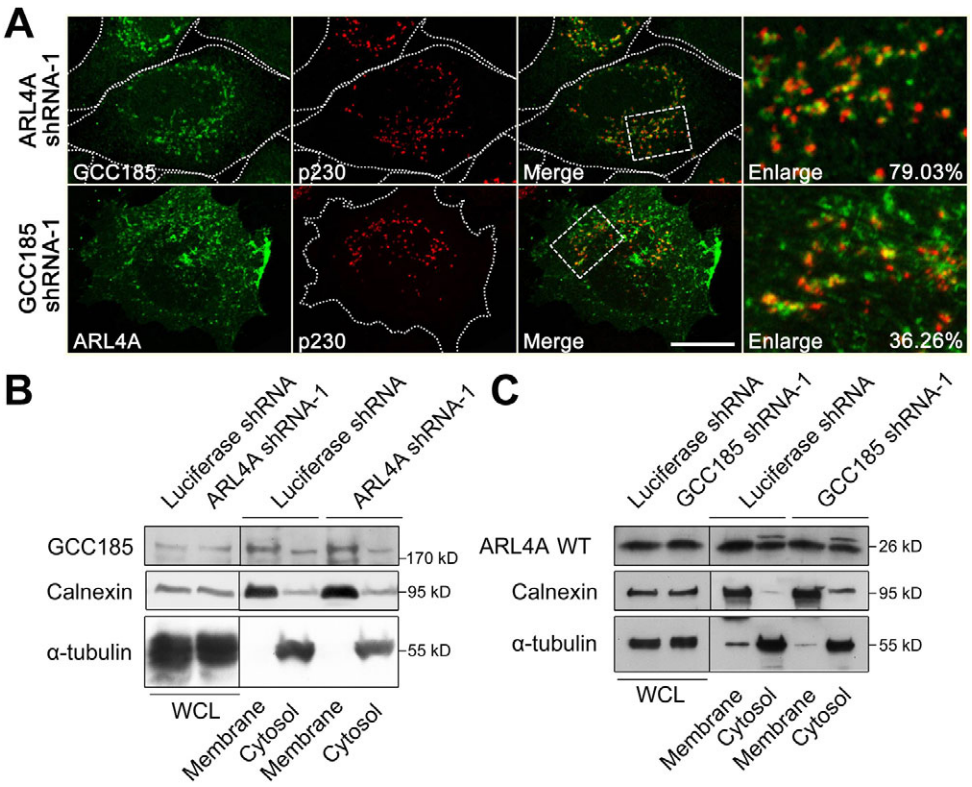

Fig. 6. The localization of GCC185 to the Golgi is ARL4A independent and vice versa. (**A**) The localization of ARL4A and GCC185 in GCC185- and ARL4A-depleted cells, respectively. HeLa cells were transfected with *ARL4A* shRNA-1 or *GCC185* shRNA-1 and subjected to puromycin selection for 72 hours. After 48 hours of shRNA transfection, GCC185-depleted cells were transfected with constructs encoding ARL4A WT. Cells were then fixed, permeabilized and processed for staining with antibodies against ARL4A or GCC185. Magnified views of the boxed regions of the merged images are shown on the right. Scale bar: 15 μm. (**B**,**C**) The subcellular distribution of GCC185 and ARL4A in ARL4A- and GCC185-depleted cells, respectively, was evaluated by fractionation. The membrane and cytosolic fractions of ARL4A- or GCC185-depleted cells were prepared as described in Materials and Methods. Ten percent of the whole cell lysates (WCL) was loaded to show expression levels.

fractionation (Fig. 8). Depletion of ARL4A or GCC185 led to exclusion of CLASPs from the Golgi (Fig. 8A); by contrast, the distribution of CLASPs did not obviously change in ARL4D-depleted cells (Fig. 8A). Subcellular fractionations showed that GCC185 depletion and ARL4A depletion lead to exclusion of CLASPs from the membrane fraction, compared with control cells (Fig. 8B). These data suggest that ARL4A, like GCC185, is required for the recruitment of CLASPs to the Golgi membrane.

We next determined whether the interaction of ARL4A and GCC185 is required for GCC185–CLASP complex formation and recruitment of CLASPs to the Golgi membrane. As shown in Fig. 9A, GCC185 depletion led to exclusion of CLASPs from the Golgi. Overexpression of exogenous GCC185FL, but not GCC185ΔCC2b, in GCC185-depleted cells recruited CLASPs to the Golgi, indicating that the ARL4A-binding domain of GCC185 is required for recruitment of CLASPs to the Golgi membrane. We next examined whether ARL4A interacts with GCC185–CLASPs complex. As shown in Fig. 9B, endogenous GCC185 and CLASPs were co-immunoprecipitated with ARL4A Q79L, indicating that ARL4A interacts with GCC185 and CLASPs in vivo. We further examined whether the interaction between GCC185 and CLASPs requires ARL4A. Endogenous CLASPs were co-immunoprecipitated with endogenous GCC185 in control cells, but to a 73% reduction in ARL4A-depleted cells (Fig. 9C). We also examined whether overexpression of ARL4A Q79L or ARL4A T34N affects the GCC185–CLASPs interaction. As shown in Fig. 9D, overexpression of ARL4A Q79L, but not of ARL4A T34N, enhances the GCC185–CLASPs interaction, suggesting that ARL4A is a positive regulator of GCC185–CLASP complexes. Taken together, we suggest that ARL4A is involved in GCC185-dependent recruitment of CLASPs to the Golgi through promoting interaction between GCC185 and CLASPs, and thus regulates the morphology of the Golgi complex.

Discussion

We present new roles of ARL4A in maintenance of Golgi structure and distinct endosome-to-Golgi transport. Several lines of evidence suggest that ARL4A interacts with GCC185 to modulate the structural integrity of the Golgi. First, ARL4A directly interacts with GCC185 in a GTP-dependent manner. Second, silencing ARL4A expression leads to the fragmentation of the Golgi complex. Third, deletion of the ARL4A-interacting region of GCC185 results in loss of maintenance of the Golgi and recruitment of CLASPs to the Golgi. Finally, the interaction between GCC185 and CLASPs is abolished upon depletion of ARL4A. From our results, we postulate that ARL4A acts as a positive modulator of GCC185–CLASPs interaction, representing a new regulatory mechanism for the organization of the Golgi complex.

We have shown that ARL4A, but not ARL4C or ARL4D, interacts with GCC185 in a GTP-dependent manner (Fig. 1B), suggesting that ARL4A has a distinct physiological role at specific organelles. The specificity of the interaction between ARL4A and GCC185 is supported by the following facts: (1) immunofluorescence microscopy showed that ARL4A, but not ARL4C or ARL4D, localize to the TGN (supplementary material Fig. S1); (2) a very low level of colocalization between ARL4C or ARL4D and GCC185 was observed in cells (Fig. 3); and (3), co-immunoprecipitation assays suggested that ARL4A, but not ARL4D, interacts with GCC185 in vivo (Fig. 1D). Taken together, these data confirmed that ARL4A is the only member of the ARL4 subfamily that is able to interact with GCC185.

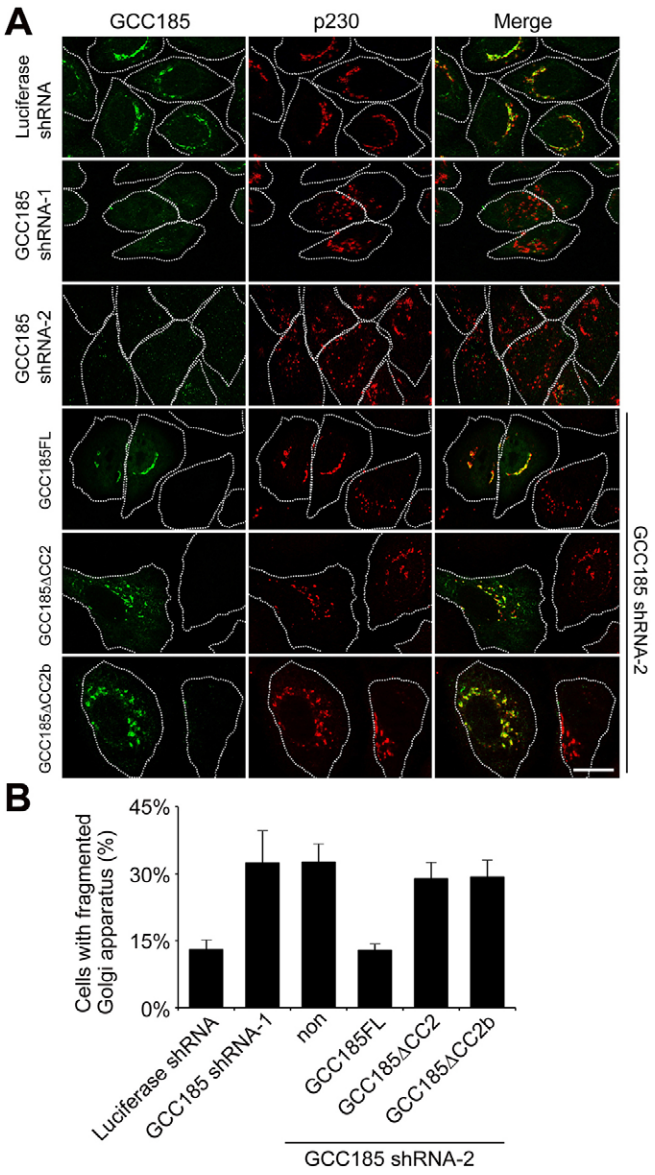

Fig. 7. The ARL4A-binding domain within GCC185 is required for the maintenance of Golgi structure. (**A**) Cells were transfected with *GCC185* shRNA-1 or *GCC185* shRNA-2 and subjected to puromycin selection for 72 hours. After 48 hours of shRNA treatment, *GCC185* shRNA-2-transfected cells were transfected with plasmids encoding the indicated proteins. Golgi localization was detected using rabbit or mouse anti-p230 antibodies. Endogenous GCC185 and exogenous GCC185 were detected using anti-GCC185 antibodies and anti-myc antibodies, respectively. Scale bar: 20 μm. (**B**) Quantification of the data shown in A. Values are means ± s.d. of three independent experiments.

The coiled-coil structure is important for the interaction between golgins and their binding partners (Hayes et al., 2009). We showed that the CC2 domain, but not the other CC domains within GCC185, was able to interact with ARL4A (Fig. 1). When the GCC185 CC2 domain sequence is aligned with the protein sequences of three other golgins, p230/golgin-245, golgin-97 and GCC88, there is no sequence similar to the GCC185 CC2 domain within the other golgins (data not shown). Using ARL4A Q79L as bait in yeast two-hybrid assay, we identified more than ten putative effectors, which did not include any golgins other than GCC185. Moreover, we found that GST–ARL4A Q79L pulled down endogenous GCC185, but not p230 or golgin-97 (our unpublished data). Thus, we suggest that ARL4A interacts with GCC185 but not with the other three TGN golgins.

The localization of GCC185 to the Golgi has been proposed to be dependent on Rab6 and Arl1 (Burguete et al., 2008); however, another study showed that the Golgi recruitment of endogenous GCC185 is independent of these two small G proteins in vivo (Houghton et al., 2009). There are several examples of golgins that do not require a Rab protein for their steady-state localization. For example, Rab9, which interacts with GCC185, was not required for Golgi localization of GCC185 (Reddy et al., 2006). Our data showed that deletion of the CC2 domain of GCC185 did not affect the Golgi localization of GCC185, which is consistent with previous studies showing that the GRIP domain, rather than the coiled-coil regions, of GCC185 is required for its Golgi localization (Barr, 1999; Kjer-Nielsen et al., 1999; Munro and Nichols, 1999; Gleeson et al., 2004). In addition, depletion of ARL4A did not affect the Golgi localization of GCC185 (Fig. 6). Thus, the identity of the interacting protein(s) responsible for the TGN localization of GCC185 remains unclear. Although ARL4A localized in a GCC185-positive subdomain (Fig. 3), deletion of GCC185 did not affect the localization of ARL4A to the Golgi (Fig. 6), which suggests that GCC185 is not required for the maintenance of the subdomain where ARL4A localizes.

A previous study showed that GCC185 constructs lacking the CC1 domain or both the CC1 and CC2 domains were not able to rescue the fragmented Golgi upon *GCC185* siRNA treatment, whereas a construct that lacked 20 residues in the middle of the CC3 domain rescued the phenotype to the same extent as the wild-type domain (Hayes et al., 2009). These results suggest that the CC1 and CC2 domains, but not CC3 domain, are required for maintenance of Golgi structure. We showed that an ARL4A binding site located in the CC2 domain of GCC185 is required for maintenance of Golgi structure and Golgi recruitment of CLASPs (Figs 4, 8).

Our study suggests that ARL4A is a low-abundance protein in cells. How can the low expression level of ARL4A support the interaction of two abundant proteins, GCC185 and CLASP? We propose a model in which the activated, GTP-bound form of ARL4A can interact with GCC185 to facilitate recruitment of CLASPs to the Golgi. After forming complexes with CLASPs, the conformation of GCC185 might be changed and a putative ARL4A GTPase-activating protein (GAP) hydrolyzes GTP so that ARL4A dissociates from GCC185. The free ARL4A protein can then recycle and be activated and interact with additional GCC185 molecules to initiate the Golgi recruitment of CLASPs (supplementary material Fig. S8). Several small GTPases, such as Rab6 and Rab9, have been identified as interacting with GCC185 (Burguete et al., 2008). Although ARL4A might not be as abundant as Rab6 or Rab9 in cells, our preliminary data show that the interaction between GCC185 and ARL4A is much stronger than the GCC185–Rab6 or GCC185–Rab9 interaction (our unpublished data). Consistent with the notion that small GTPases function as molecular switches by turning on the subsequent events (Goud and Gleeson, 2010), we reason that even a small amount of ARL4A can interact with GCC185 more efficiently than Rab6 or Rab9. Interestingly, a previous study showed that CLASP1 function is also regulated through its

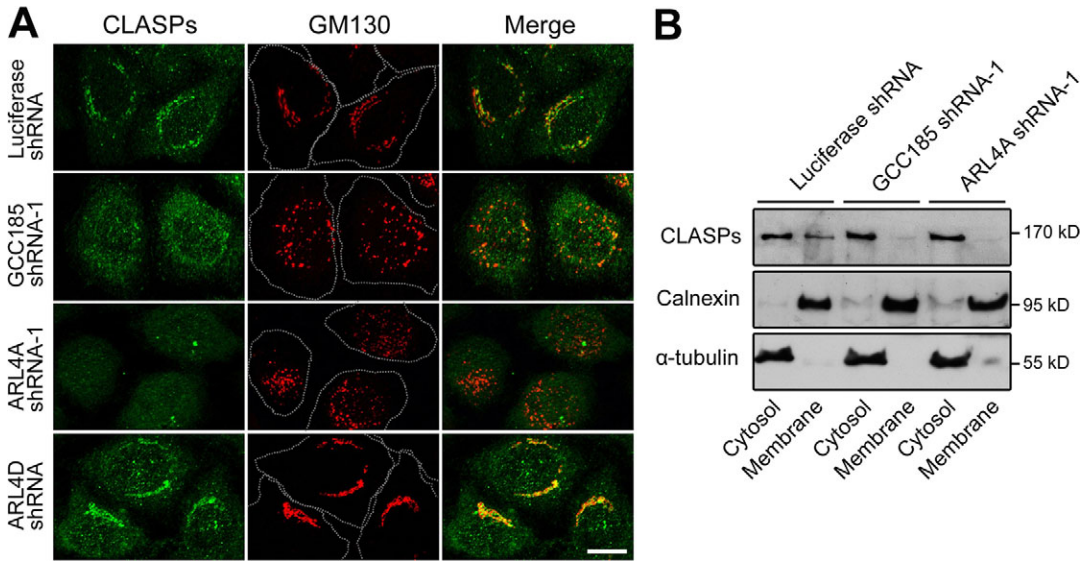

Fig. 8. Depletion of either ARL4A or GCC185 leads to exclusion of CLASPs from the Golgi. (**A**) HeLa cells were transfected with the indicated shRNA constructs and grown for 72 hours under puromycin selection. Transfected cells were fixed and stained with a polyclonal rabbit anti-CLASPs antibody and a mouse monoclonal anti-GM130 antibody, followed by the appropriate Alexa-Fluor-conjugated secondary antibodies. Scale bar: 15 μm. (**B**) The subcellular distribution of endogenous CLASPs. Cytosolic and membrane fractions of HeLa cells were prepared as described in the Materials and Methods. Equivalent amounts of proteins were analyzed by immunoblotting with specific antibodies against CLASPs, α-tubulin (cytosol marker) and calnexin (membrane marker).

interaction with a low-abundance protein, KIF2b, which is transiently recruited and concentrated to the kinetochores (Manning et al., 2010). Our study found that ARL4A functions and interacts with GCC185 in a nucleotide-dependent manner (Figs 1, 3, Fig. 4C), which suggests that a putative guanine-nucleotide exchange factor (GEF) and GAP of ARL4A play important roles in regulating the interaction between ARL4A and GCC185. Identification of the upstream molecules of ARL4A, such as ARL4A GAP and GEF, is of great importance to further explore the detailed mechanism.

We have shown that depletion of ARL4A disrupts CCC185–CLASPs interaction and leads to Golgi fragmentation (Figs 4, 9). Therefore, overexpression of ARL4A Q79L strengthens the GCC185–CLASPs interaction, which implies that it affects Golgi structure (Fig. 9D). However, overexpression of ARL4A Q79L did not dramatically affect Golgi structure (supplementary material Fig. 1B). The structural integrity of the Golgi complex is known to be dependent upon microtubule polymerization and microtubule–Golgi interaction (Goud and Gleeson, 2010). In addition to these events, several factors such as motor proteins and centrosome-derived microtubules, are also required for the maintenance of Golgi structure (Thyberg and Moskalewski, 1999). Overexpression of ARL4A might not be sufficient to dramatically affect Golgi structure, suggesting that many regulators are needed to modulate the function of GCC185. Similarly, neither the overexpression of GCC185 nor that of CLASPs affects Golgi structure (supplementary material Fig. S6B) (Efimov et al., 2007).

Retrograde transport pathways that move proteins from early/recycling endosomes to the TGN are important for the recycling of endogenous cargos (Johannes and Popoff, 2008). The molecular requirements for toxins, M6PR and other retrograde cargoes were defined by different factors. Of particular note are TGN golgins (Johannes and Popoff, 2008). Golgin-97 is important for both CTxB and STxB retrograde transport (Lu et al., 2004) and p230/golgin-245 modulates STxB transport from endosomes to the Golgi (Yoshino et al., 2005). Depletion of GCC185 disrupted Golgi structure and inhibited the retrograde trafficking of STxB and M6PR, but not TGN38 or CTxB (Reddy et al., 2006; Derby et al., 2007; Ganley et al., 2008). The retrograde transport of TGN38 and STxB differs in the requirement for GCC88 and GCC185, respectively (Lieu and Gleeson, 2010). Our findings indicate that ARL4A, like GCC185, is required for distinct endosome-to-Golgi transport but not for endocytosis from plasma membrane to endosomes. How does ARL4A affect GCC185-mediated transport from endosomes to the TGN? It is possible that GCC185-dependent endosome-to-Golgi transport requires the interaction of ARL4A-containing transport vesicles with GCC185 through its CC2 domain, as supported by the of 37 residues in the CC2b region, which impairs GCC185-mediated transport of M6PR (supplementary material Fig. S7). Another scenario is that the Golgi-associated ARL4A interacts with the CC2 domain to mediate a tethering conformation of GCC185 on the TGN. Perhaps this ARL4A–GCC185 tethering conformation facilitates transport vesicle docking and fusion. However, CC2b deletion might abolish the interaction not only with ARL4A, but also with other GCC185 binding partners, resulting in defects in interaction between transport vesicles and GCC185. An important challenge for the future will be to determine how GCC185 binding to ARL4A enables specific endosomal vesicles to dock productively at the TGN.

In summary, our results showed that GCC185 is an ARL4A effector and highlight a complex role for the ARL4A–GCC185 interaction in the emerging relationship between maintenance of Golgi structure and retrograde transport. Defining the molecular mechanism of how ARL4A promotes interaction between GCC185 and the CLASPs in vivo will require considerable further work. Analysis of ‘upstream’ regulators of ARL4A that underlie its selective recruitment to and activity at the TGN will

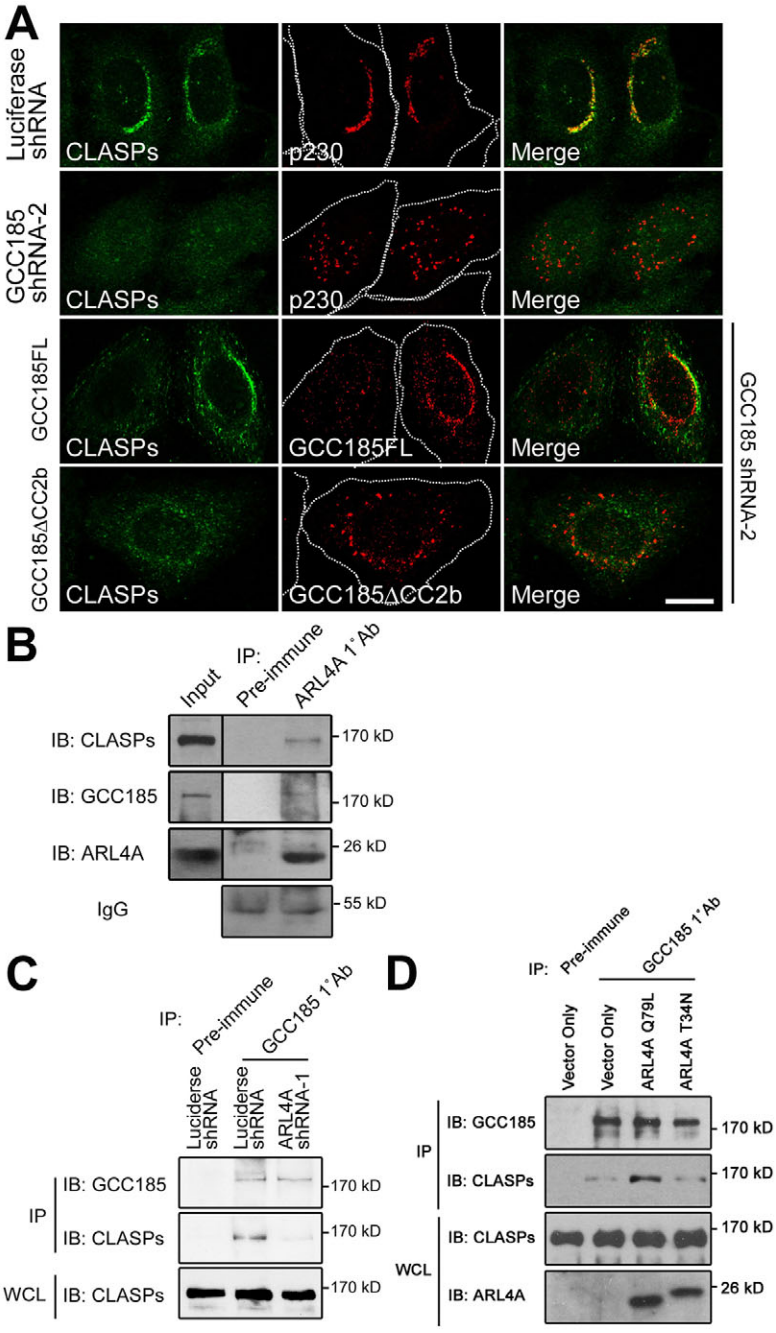

Fig. 9. ARL4A is required for GCC185-mediated Golgi recruitment of CLASPs. (**A**) The ARL4A-binding domain in GCC185 is required for Golgi recruitment of CLASPs. Cells were transfected with *GCC185* shRNA-2 and grown under puromycin selection for 72 hours. After 48 hours of shRNA transfection, cells were transfected with plasmids encoding GCC185FL or GCC185ΔCC2b. Endogenous CLASPs were detected using an antibody against CLASPs. Endogenous GCC185 and exogenous GCC185 were detected using an anti-GCC185 antibody and an anti-myc antibody, respectively. Scale bar: 15 μm. (**B**) Interaction between ARL4A, GCC185 and CLASPs in vivo. HeLa cells expressing ARL4A Q79L were lysed and incubated with equal amounts of preimmune serum, or anti-ARL4A antibody. Immune complexes were isolated using protein-A–Sepharose, and bound proteins were analyzed by immunoblotting with anti-GCC185, anti-ARL4A or anti-CLASPs antibody. Ten percent of each cell lysate (input) was loaded to show expression levels. (**C**) Depletion of ARL4A abolishes the interactions between GCC185 and CLASPs. HEK293T cells were transfected with control luciferase or *ARL4A* shRNA-1 and grown for 72 hours. Transfected cells were lysed and incubated with equal amounts of preimmune serum or anti-GCC185 antibody. Immune complexes were isolated using protein-A–Sepharose, and bound proteins were analyzed by SDS-PAGE and immunoblotting with anti-GCC185 and anti-CLASP antibodies. Ten percent of the whole cell lysates (WCL) was loaded to show the expression levels of the CLASPs. (**D**) Overexpression of ARL4A Q79L, but not of ARL4A T34N, enhances the GCC185–CLASPs interaction. Vector-transfected control cells and the indicated ARL4A-transfected cells were lysed and incubated with equal amounts of preimmune serum or anti-GCC185 antibody. Immune complexes were isolated using protein-A–Sepharose, and bound proteins were analyzed by SDS-PAGE and immunoblotting with anti-GCC185 and anti-CLASPs antibodies. Ten percent of the whole cell lysates (WCL) was loaded to show the expression levels of the CLASPs and ARL4A.

improve our understanding of the new mechanism of ARL4A in regulating Golgi organization.

Materials and Methods

Antibodies

The polyclonal antibodies against ARL4A, ARL4C and ARL4D used in this study have been previously described (Lin et al., 2002; Li et al., 2007). The polyclonal antibody against GCC185 was developed by immunizing rabbits with a purified recombinant His-tagged GCC185 fragment (residues 414–733). The mouse monoclonal antibodies used were: His, Rab6, HA (Santa Cruz Biotechnology, Inc.), myc (BAbCO), Rab9 (Calbiochem), calnexin, GM130, p230, LAMP1, cytochrome *c*, EEA1, TGN38, syntaxin-6 (BD), α-tubulin (Sigma-Aldrich), M6PR, pan-cadherin (Abcam) and transferrin receptor (Molecular Probes). Horseradish peroxidase-conjugated sheep anti-rabbit, anti-mouse and anti-rat immunoglobulin (IgG) antibodies were from GE Healthcare. Alexa-Fluor-594-, -488- or -350-conjugated anti-rabbit, anti-mouse and anti-rat antibodies were obtained from Invitrogen. We gratefully thank Chia-Jung Yu (Chang Gung University, Taiwan) for the rabbit polyclonal antibody against p230 and Irina Kaverina (Vanderbilt University Medical Center, Nashville, TN) for the rabbit polyclonal antibody against CLASPs. The antibody for immunostaining CLASPs had been previously described [#KT68; ABsea (Maffini et al., 2009)]. The staining of a ~160 kDa protein was abolished by co-transfection of *CLASP1* shRNA and *CLASP2* shRNA (supplementary material Fig. S2D). Fluorescein-conjugated M6PR antibodies were prepared using a Lightning-Link fluorescein Conjugation Kit (Innova Biosciences) according to the manufacturer's protocol.

Plasmids

Wild-type *ARL4A*, *ARL4C* and *ARL4D* cDNAs, and their mutants (Li et al., 2007) were subcloned into the pSG5 vector (Stratagene). The pSG5–ARL4A WT construct was mutagenized by polymerase chain reaction (PCR) to generate shRNA-resistant pSG5–ARL4A WT, pSG5–ARL4A Q79L and pSG5–ARL4A T34N, which contained three silent mutations introduced into the region targeted

by *ARL4A* shRNA-2. For the full-length GCC185 expression construct, residues 1-408 and 409-1684 of *GCC185* were amplified from a HeLa cells cDNA pool and pBluescript-SK$^+$-KIAA0336 (Supplier, Kisarasu, Japan), respectively, and plasmids were constructed by inserting the two PCR-amplified products into pcDNA3.1B (Invitrogen). To introduce deletion mutations, the ΔCC2 (deletion of residues 394–751) and CC2Δb (deletion of residues 512–549), into GCC185, a two-step recombinant PCR procedure was used, and then subcloned PCR products into pcDNA3.1B. For the yeast two-hybrid assay, the following domains of GCC185, amplified from the pcDNA3.1B–GCC185FL, were subcloned into the yeast prey vector pACT2 (Clontech): CC1 (residues 34–358), CC2 (residues 394–751), GCC185(500–714), GCC185(500–714) Δb (deletion of residues 500–549), GCC185(500–714) Δc (deletion of residues 575–614), GCC185(500–714) Δd (deletion of residues 633–670), GCC185(500–714) Δe (deletion of residues 671–714), CC3 (residues 805–889), C-terminal domain (residues 811–1684) and C270 (residues 1415–1684). ARL4A, ARL4C, ARL4D and their mutants were subcloned into bait vector pBTM116 (Clontech). For the GST pull-down assay, ARL4A Q79L was subcloned into pGEX4T-1 (GE Healthcare); CC2, C27 and CC2Δb (residues 394–751; deletion of residues 512–549) were subcloned into pET32a (Novagen). TGN38 was amplified from rat cDNA and subcloned into pEGFP/N2 vector (Clontech). The LAMP1–RFP construct and dsRed–mem construct were purchased from Addgene and Clontech, respectively. Vesicular stomatitis virus glycoprotein (VSVG)–GFP was a gift from Jennifer Lippincott-Schwartz (National Institutes of Health, Bethesda, MD). shRNAs were expressed in the pLKO-1 vector containing a puromycin-resistant cassette or a GFP-expression cassette and were obtained from National RNAi Core Facility in Taiwan. The following shRNA sequences were used: luciferase shRNA: 5′-CCTAAGGTTAAGTCGCCCTCG-3′; *ARL4A* shRNA-1: 5′-CAGTCTTTCCAC-ATTGTTATT-3′; *ARL4A* shRNA-2: 5′-ACAAGATTTGAGGAACTCATT-3′; *GCC185* shRNA-1: 5′-GAGAGCAGAGTTGATACTATT-3′; *GCC185* shRNA-2: 5′-GCTGACATGAAGAGTTTAGTT-3′; *ARL4D* shRNA: 5′-CGCCTCAAGTT-CAAGGAGTTT-3′; *CLASP1* shRNA: 5′-CCCTTTATTTATCAAGCGTAA-3′; *CLASP2* shRNA: 5′-GCCAGTGTTATGATTGTATAA-3′. All constructs and mutants were confirmed by DNA sequencing.

Cell culture and transfection

HeLa cells or HEK293T cells were maintained in DMEM supplemented with 10% fetal bovine serum (Hyclone Laboratories), penicillin (Sigma-Aldrich) and streptomycin (Invitrogen) in a humidified incubator with 5% CO_2 at 37℃. Transient transfection was performed using the Lipofectamine 2000 reagent according to the manufacturer's protocol (Invitrogen). Cells were harvested 24–72 hours after transfection. After pLKO-1-based shRNA transfection for 24 hours, puromycin (2 μg/ml; Sigma-Aldrich) was added and cells were incubated for an additional 48 hours to enrich the transfected cells.

Yeast two-hybrid screen and interaction assay

The yeast two-hybrid screen and interaction assay was performed essentially as described previously (Li et al., 2007). A human fetal brain cDNA library in pACT2 (Clontech) was screened using ARL4A Q79L as bait. For histidine auxotrophy and β-galactosidase expression, we screened 3.2×10^6 clones and obtained clones that specifically interacted with ARL4A Q79L.

In vitro binding assay

Induction and purification of His- or GST-tagged fusion proteins were performed essentially as described previously (Li et al., 2007). Purified GST or GST–ARL4A Q79L bound to glutathione–Sepharose beads (GE Healthcare) was incubated with purified recombinant CC2–His, C270–His or CC2Δb–His in binding buffer (1% bovine serum albumin, 50 mM KCl, 100 mM NaCl, 2 mM $CaCl_2$, 2 mM $MgCl_2$, 5 mM dithiothreitol, 50 mM Tris, pH 7.5, and protease inhibitors) overnight at 4℃. After incubation, the beads were washed five times with binding buffer containing 0.05% Tween 20. Bound proteins were eluted, denatured in SDS sample buffer, and analyzed by immunoblotting.

In vivo pull-down assay

HEK293T cells expressing GCC185FL or GCC185ΔCC2b were lysed by sonication on ice in lysis buffer (150 mM NaCl, 1% NP-40, 50 mM Tris-HCl) containing protease inhibitors. The lysates were collected after removal of cell debris by centrifugation (12,000 ***g*** for 10 minutes at 4℃) and then incubated with 1 μg GST or GST–ARL4A Q79L bound to glutathione–Sepharose for 2 hours at 4℃. After the glutathione–Sepharose was washed three times with lysis buffer, the bound proteins were eluted and analyzed by SDS-PAGE and immunoblotting.

Co-immunoprecipitation

HeLa cells or HEK293T cells were treated with 2 mM dithiobis succinimidylpropionate (DSP; Pierce) for 15 minutes, and lysed in lysis buffer (150 mM NaCl, 1% NP-40, 50 mM Tris-HCl) containing protease inhibitors. Lysates were cleared by centrifugation (12,000 ***g*** for 15 minutes at 4℃) and incubated with the indicated antibodies at 4℃ for 2 hours. The mixture of cell lysates and antibodies were incubated with protein-A–Sepharose (GE Healthcare) overnight at 4℃ with rocking. After three washes of the Sepharose with lysis buffer, the co-immunoprecipitated proteins were eluted and analyzed by SDS-PAGE and immunoblotting.

Immunofluorescence microscopy and immunoblotting

Cells grown on coverslips were fixed in 4% formaldehyde for 15 minutes at room temperature. After washing with PBS, the cells were permeabilized using 0.01% Triton X-100 in PBS for 5 minutes. For immunostaining of CLASPs, the cells were fixed in cold methanol at −20℃ for 10 minutes and then treated for 1 minute with methanol–acetone (1:1 mixture). After two washes with PBS, the cells were incubated in blocking buffer (0.1% saponin, 0.2% BSA) for 30 minutes at room temperature. Following blocking, cells were incubated with primary antibodies in blocking buffer for 1 hour and then incubated with Alexa-Fluor-conjugated secondary antibodies (Molecular Probes) for 1 hour. After washing with PBS, the cells were mounted and finally visualized using an Axioplan 2 microscope (Carl Zeiss, Inc.). The images were taken using the apotome mode for optical sectioning, and stacked images were reconstructed using Axiovision 4.7 software (Carl Zeiss, Inc.). Immunoblot analyses of proteins were performed as previously described (Li et al., 2007).

STxB and CTxB internalization assay

Cy3-conjugated STxB was prepared as previously described (Tai et al., 2005). Cells were incubated in DMEM containing Cy3-conjugated STxB or Alexa-Fluor-594-conjugated CTxB (4 μg/ml; Molecular Probes) at 4℃ for 30 minutes. After washing with ice-cold DMEM, internalization was initiated by shifting the incubation temperature to 37℃; the labeled STxB or CTxB was then chased for 40 minutes. Thereafter, the cells were fixed and subjected to immunostaining. The Alexa-Fluor-488−transferrin (Molecular Probes) uptake assay has been previously described (Mallard et al., 1998).

TGN38 trafficking assay

The TGN38 trafficking assay was performed as previously described (Derby et al., 2007). GFP−TGN38 and pLKO-1-based shRNA co-transfected cells were incubated with anti-rat TGN38 antibody (1.25 μg/ml; BD Biosciences) on ice for 30 minutes. Unbound antibodies were removed by washing with serum-free medium, and the internalization of antibody-bound TGN38 was allowed to progress at 37℃ for 120 minutes. Cells were fixed and the internalized TGN38–antibody complexes were detected using appropriate secondary antibodies.

VSVG transport

The VSVG transport assay was performed as previously described (Scales et al., 1997). Briefly, VSVG−GFP and pLKO-1-based shRNA co-transfected cells were incubated in a humidified incubator with 5% CO_2 at 39.5℃ overnight, and then treated with cycloheximide (100 μg/ml; Merck) at 32℃ for 120 minutes. Finally, cells were fixed for staining with anti-p230 antibodies, followed by appropriate secondary antibodies.

Subcellular fractionation

The cytosol–membrane fractionations were performed as previously described (Li et al., 2007). HeLa cells were transfected with different pLKO-1-based shRNA constructs, treated with puromycin, and membrane and cytosolic fractions were then prepared using a CNM compartment protein extraction kit (BioChain Institute, Inc. 3507 Breakwater Ave., Hayward, CA 94545, USA) according to the manufacturer's protocol.

Quantitative real-time PCR

Total RNA isolated from HeLa cells was used to synthesize first-strand cDNA, and then amplified by PCR. Primers were as follows: ARL4A forward, 5′-ATG-GGGAATGGGCTGTCAGA-3′, and reverse, 5′-TCATCTTTTCTTTTTCTGT-TGCCGC-3′; β-actin forward, 5′-ATCATGTTTGAGACCTTCAA-3′, and reverse, 5′-CATCTCTTGCTCGAAGTCCA-3′. The amplified products were checked using agarose gel (supplementary material Fig. S2A). Quantitative real-time PCR was performed using SYBR Green Master Mix (Fermentas) in the 7900HT Fast Real-time PCR system (Applied Biosystems).

Acknowledgements

We thank Irina Kaverina for providing the CLASPs antibodies, Chia-Jung Yu for the polyclonal p230 antibodies, Dr Jennifer Lippincott-Schwartz for the VSVG–GFP plasmid and Ludger Johannes for the STxB plasmid. We also thank Joel Moss, Randy Haun and Chun-Fang Huang for critical review of this manuscript.

Funding

This work was supported by grants from the National Science Council, Taiwan [grant number NSC-97-3112-B-002-016-PAE to F.-J.L.];

National Taiwan University Hospital [grant numbers 97A08-1, 98P26-1, 99P21-1 to F.-J.L.]; and the Yung-Shin Biomedical Research Funds [grant number YSP-86-019 to F.-J.L.].

Supplementary material available online at
http://jcs.biologists.org/lookup/suppl/doi:10.1242/jcs.086892/-/DC1

References

Barr, F. A. (1999). A novel Rab6-interacting domain defines a family of Golgi-targeted coiled-coil proteins. *Curr. Biol.* **9**, 381-384.

Burd, C. G., Strochlic, T. I. and Gangi Setty, S. R. (2004). Arf-like GTPases: not so Arf-like after all. *Trends Cell Biol.* **14**, 687-694.

Burguete, A. S., Fenn, T. D., Brunger, A. T. and Pfeffer, S. R. (2008). Rab and Arl GTPase family members cooperate in the localization of the golgin GCC185. *Cell* **132**, 286-298.

D'Souza-Schorey, C. and Chavrier, P. (2006). ARF proteins: roles in membrane traffic and beyond. *Nat. Rev. Mol. Cell Biol.* **7**, 347-358.

Derby, M. C., Lieu, Z. Z., Brown, D., Stow, J. L., Goud, B. and Gleeson, P. A. (2007). The trans-Golgi network golgin, GCC185, is required for endosome-to-Golgi transport and maintenance of Golgi structure. *Traffic* **8**, 758-773.

Efimov, A., Kharitonov, A., Efimova, N., Loncarek, J., Miller, P. M., Andreyeva, N., Gleeson, P., Galjart, N., Maia, A. R., McLeod, I. X. et al. (2007). Asymmetric CLASP-dependent nucleation of noncentrosomal microtubules at the trans-Golgi network. *Dev. Cell* **12**, 917-930.

Ganley, I. G., Espinosa, E. and Pfeffer, S. R. (2008). A syntaxin 10-SNARE complex distinguishes two distinct transport routes from endosomes to the trans-Golgi in human cells. *J. Cell Biol.* **180**, 159-172.

Ghosh, P., Dahms, N. M. and Kornfeld, S. (2003). Mannose 6-phosphate receptors: new twists in the tale. *Nat. Rev. Mol. Cell Biol.* **4**, 202-212.

Gleeson, P. A., Lock, J. G., Luke, M. R. and Stow, J. L. (2004). Domains of the TGN: coats, tethers and G proteins. *Traffic* **5**, 315-326.

Goud, B. and Gleeson, P. A. (2010). TGN golgins, Rabs and cytoskeleton: regulating the Golgi trafficking highways. *Trends Cell Biol.* **20**, 329-336.

Hayes, G. L., Brown, F. C., Haas, A. K., Nottingham, R. M., Barr, F. A. and Pfeffer, S. R. (2009). Multiple Rab GTPase binding sites in GCC185 suggest a model for vesicle tethering at the trans-Golgi. *Mol. Biol. Cell* **20**, 209-217.

Hofmann, I., Thompson, A., Sanderson, C. M. and Munro, S. (2007). The Arl4 family of small G proteins can recruit the cytohesin Arf6 exchange factors to the plasma membrane. *Curr. Biol.* **17**, 711-716.

Houghton, F. J., Chew, P. L., Lodeho, S., Goud, B. and Gleeson, P. A. (2009). The localization of the Golgin GCC185 is independent of Rab6A/A' and Arl1. *Cell* **138**, 787-794.

Johannes, L. and Popoff, V. (2008). Tracing the retrograde route in protein trafficking. *Cell* **135**, 1175-1187.

Kjer-Nielsen, L., Teasdale, R. D., van Vliet, C. and Gleeson, P. A. (1999). A novel Golgi-localisation domain shared by a class of coiled-coil peripheral membrane proteins. *Curr. Biol.* **9**, 385-388.

Li, C. C., Chiang, T. C., Wu, T. S., Pacheco-Rodriguez, G., Moss, J. and Lee, F. J. (2007). ARL4D recruits cytohesin-2/ARNO to modulate actin remodeling. *Mol. Biol. Cell* **18**, 4420-4437.

Lieu, Z. Z. and Gleeson, P. A. (2010). Identification of different itineraries and retromer components for endosome-to-Golgi transport of TGN38 and Shiga toxin. *Eur. J. Cell Biol.* **89**, 379-393.

Lin, C. Y., Huang, P. H., Liao, W. L., Cheng, H. J., Huang, C. F., Kuo, J. C., Patton, W. A., Massenburg, D., Moss, J. and Lee, F. J. S. (2000). ARL4, an ARF-like protein that is developmentally regulated and localized to nuclei and nucleoli. *J. Biol. Chem.* **275**, 37815-37823.

Lin, C. Y., Li, C. C., Huang, P. H. and Lee, F. J. S. (2002). A developmentally regulated ARF-like 5 protein (ARL5), localized to nuclei and nucleoli, interacts with heterochromatin protein 1. *J. Cell Sci.* **115**, 4433-4445.

Lu, L., Tai, G. and Hong, W. (2004). Autoantigen Golgin-97, an effector of Arl1 GTPase, participates in traffic from the endosome to the trans-golgi network. *Mol. Biol. Cell* **15**, 4426-4443.

Maffini, S., Maia, A. R., Manning, A. L., Maliga, Z., Pereira, A. L., Junqueira, M., Shevchenko, A., Hyman, A., Yates, J. R., 3rd, Galjart, N. et al. (2009). Motor-independent targeting of CLASPs to kinetochores by CENP-E promotes microtubule turnover and poleward flux. *Curr. Biol.* **19**, 1566-1572.

Mallard, F., Antony, C., Tenza, D., Salamero, J., Goud, B. and Johannes, L. (1998). Direct pathway from early/recycling endosomes to the Golgi apparatus revealed through the study of shiga toxin B-fragment transport. *J. Cell Biol.* **143**, 973-990.

Manning, A. L., Bakhoum, S. F., Maffini, S., Correia-Melo, C., Maiato, H. and Compton, D. A. (2010). CLASP1, astrin and Kif2b form a molecular switch that regulates kinetochore-microtubule dynamics to promote mitotic progression and fidelity. *EMBO J.* **29**, 3531-3543.

Miller, P. M., Folkmann, A. W., Maia, A. R., Efimova, N., Efimov, A. and Kaverina, I. (2009). Golgi-derived CLASP-dependent microtubules control Golgi organization and polarized trafficking in motile cells. *Nat. Cell Biol.* **11**, 1069-1080.

Munro, S. and Nichols, B. J. (1999). The GRIP domain – a novel Golgi-targeting domain found in several coiled-coil proteins. *Curr. Biol.* **9**, 377-380.

Reddy, J. V., Burguete, A. S., Sridevi, K., Ganley, I. G., Nottingham, R. M. and Pfeffer, S. R. (2006). A functional role for the GCC185 golgin in mannose 6-phosphate receptor recycling. *Mol. Biol. Cell* **17**, 4353-4363.

Scales, S. J., Pepperkok, R. and Kreis, T. E. (1997). Visualization of ER-to-Golgi transport in living cells reveals a sequential mode of action for COPII and COPI. *Cell* **90**, 1137-1148.

Schürmann, A., Breiner, M., Becker, W., Huppertz, C., Kainulainen, H., Kentrup, H. and Joost, H. G. (1994). Cloning of two novel ADP-ribosylation factor-like proteins and characterization of their differential expression in 3T3-L1 cells. *J. Biol. Chem.* **269**, 15683-15688.

Schürmann, A., Koling, S., Jacobs, S., Saftig, P., Krau, S., Wennemuth, G., Kluge, R. and Joost, H. G. (2002). Reduced sperm count and normal fertility in male mice with targeted disruption of the ADP-ribosylation factor-like 4 (Arl4) gene. *Mol. Cell. Biol.* **22**, 2761-2768.

Sinka, R., Gillingham, A. K., Kondylis, V. and Munro, S. (2008). Golgi coiled-coil proteins contain multiple binding sites for Rab family G proteins. *J. Cell Biol.* **183**, 607-615.

Stenmark, H. (2009). Rab GTPases as coordinators of vesicle traffic. *Nat. Rev. Mol. Cell. Biol.* **10**, 513-525.

Stephan, J., Christiane, S., Frank, F., Susanne, K., Yvonne, W., Annette, S. and Hans-Georg, J. (1999). ADP-ribosylation factor (ARF)-like 4, 6, and 7 represent a subgroup of the ARF family characterized by rapid nucleotide exchange and a nuclear localization signal. *FEBS Lett.* **456**, 384-388.

Tai, G., Lu, L., Johannes, L. and Hong, W. (2005). Functional analysis of Arl1 and Golgin-97 in endosome-to-TGN transport using recombinant Shiga Toxin B fragment. *Methods Enzymol.* **404**, 442-453

Thyberg, J. and Moskalewski, S. (1999). Role of microtubules in the organization of the Golgi complex. *Exp. Cell Res.* **246**, 263-279.

Yoshino, A., Bieler, B. M., Harper, D. C., Cowan, D. A., Sutterwala, S., Gay, D. M., Cole, N. B., McCaffery, J. M. and Marks, M. S. (2003). A role for GRIP domain proteins and/or their ligands in structure and function of the trans Golgi network. *J. Cell Sci.* **116**, 4441-4454.

Yoshino, A., Setty, S. R., Poynton, C., Whiteman, E. L., Saint-Pol, A., Burd, C. G., Johannes, L., Holzbaur, E. L., Koval, M., McCaffery, J. M. et al. (2005). tGolgin-1 (p230, golgin-245) modulates Shiga-toxin transport to the Golgi and Golgi motility towards the microtubule-organizing centre. *J. Cell Sci.* **118**, 2279-2293.